IEEE Photonics Journal
An IEEE Photonics Society Publication

Generation of Focal Patterns With Uniform Intensity Distribution From Speckle by Hadamard-Genetic Algorithm

Volume 13, Number 3, June 2021

Haoran Li
Xiaoyan Wu
Guodong Liu
Xiaoyan Wang
Songjie Luo
Ziyang Chen
Jixiong Pu

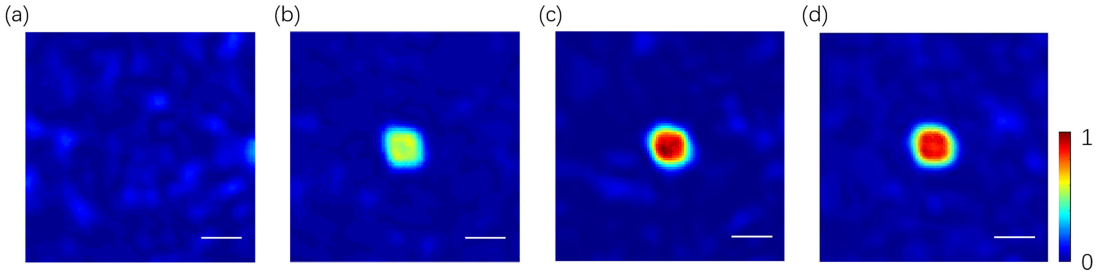

DOI: 10.1109/JPHOT.2021.3075111

Generation of Focal Patterns With Uniform Intensity Distribution From Speckle by Hadamard-Genetic Algorithm

Haoran Li,[1] Xiaoyan Wu,[2,3] Guodong Liu,[2,3] Xiaoyan Wang,[1] Songjie Luo,[1] Ziyang Chen ,[1] and Jixiong Pu [1]

[1]College of Information Science and Engineering, Fujian Key Laboratory of Light Propagation and Transformation, Huaqiao University, Xiamen, Fujian 361021, China
[2]Institute of Fluid Physics, China Academy of Engineering Physics, Mianyang 621900, China
[3]Key Laboratory of Science and Technology on High Energy Laser, China Academy of Engineering Physics, Mianyang 621900, China

DOI:10.1109/JPHOT.2021.3075111

Manuscript received March 16, 2021; revised April 16, 2021; accepted April 20, 2021. Date of publication April 23, 2021; date of current version May 17, 2021. This work was supported in part by the National Natural Science Foundation of China (NSFC) under Grants 11674111, 62005086, and in part by the Fujian Province Science Funds for Distinguished Young Scholar under Grant 2018J06017. Corresponding authors: Xiaoyan Wu and Ziyang Chen (e-mail: wuxiaoyan1219@sina.cn; ziyang@hqu.edu.cn).

Abstract: When a coherent beam transmits through a scattering medium, a random intensity distribution known as speckle is generated. Generally, such speckles can be modulated by feedback-based wavefront shaping, as exemplified by the generation of a bright focal spot. However, it is more challenging to generate a specific focal pattern with uniform intensity distribution. In this study, the Hadamard–Genetic algorithm (HGA), namely a hybrid phase modulation scheme of Hadamard encoding algorithm (HEA) and genetic algorithm (GA), is proposed to face these challenges. This algorithm takes advantages of the high intensity of HEA and the high uniformity of GA and outperforms traditional optimization schemes, especially in suppressing intensity fluctuations of the focal pattern. This research is expected to be applied in the field of laser processing and particle manipulation.

Index Terms: Wavefront shaping, speckle modulation, Hadamard-Genetic algorithm.

1. Introduction

Focal beams with designed pattern have been widely applied in areas ranging from laser processing to particle manipulation [1]–[2], such as laser fusion and optical tweezers. Laser beams with uniform intensity distribution are crucial in precise laser processing because the smoothness of processing depends on the uniformity of the intensity distribution. Although beam shape modulation in free space has been well developed, this modulation task is challenged by the presence of a scattering medium. Owing to random scattering, a seemingly-uncontrollable random distribution, known as the speckle, is generated when light beams propagate through a scattering medium. In 2007, Vellekoop and Mosk first reported that the speckle pattern can be modulated into a bright focal spot with optimized wavefront [3]. Known as feedback-based wavefront shaping, this method has been widely applied in the speckle modulation. Studies [4]–[16] have demonstrated that the

scattering medium can be treated as versatile optical elements, such as imaging lens, beam splitter, and spectrum filter.

In past decades, research on the intensity modulation of speckle pattern primarily focuses on the generation of a bright focus. Choi and van Putten broke the diffraction limit with the help of scattering medium [17]–[18]. With the increase in the diverse requirement of a uniform focal pattern in laser processing, the production of uniform focal patterns with designed shape from a speckle must be investigated. Compared with the generation of a single focal spot, in which only the intensity enhancement in a specific point is considered, the balance between the intensity enhancement and uniformity of the whole focal pattern should be also considered in the modulation of the speckle into a uniform designed pattern. Clearly, the latter consideration faces more challenges.

As a representative global optimization algorithm, the genetic algorithm (GA) has been applied in speckle modulation and has performed satisfactorily in low signal-to-noise (SNR) environment [19]. Conkey et al. designed a cost function, which depends on the enhancement and standard deviation of the intensity in the focal region, as the fitness of GA to achieve multi-point focusing [20]. However, the uniformity of the intensity distribution obtained by this method is limited, and the balance between enhancement and intensity uniformity cannot be flexibly adjusted. Pearson correlation coefficient (PCC), which describes the correlation between the modulated light field and the pre-designed pattern, has been introduced as the fitness of the GA [21]. The ineffectiveness of this scheme becomes pronounced when a large field is chosen as the target [21]. Some other methods, such as non-dominated sorting GA II with hybrid optimization scheme, have also been proposed for modulating the intensity distribution of the speckle field [22]–[23].

Hadamard encoding algorithm (HEA) has been widely used in compressed sensing and digital communication [24]–[25]. It can achieve a high SNR [26], and has been applied in suppressing the intensity of a speckle field [27]. Furthermore, this method functions suitably for modulating the wavefront to focus the scattering light into a bright focal spot [28].

In this study, HEA and GA are combined to generate designed focal patterns with high intensity and uniformity. First, the performances of HEA and GA in the generation of a uniform focal pattern are compared. A new algorithm that secures both advantages of these two algorithms is then proposed. This algorithm in modulating the speckle into a uniform focal region is examined to confirm whether it indeed outperforms previously-reported algorithms.

2. Principle of Wavefront Shaping

Consider the propagation of light through a scattering medium, if the incident light field is divided into N elements, then the transmitted field in the target, $E_m^{(out)}$, constitutes a linear combination of the fields coming from these N elements [3]:

$$E_m^{(out)} = \sum_{n=1}^{N} t_{mn} E_n^{(in)} = \sum_{n=1}^{N} t_{mn} A_n \exp(i\varphi_n), \tag{1}$$

where $E_m^{(out)}$ is the output field, $E_n^{(in)}$ is the incident field with the form of $A_n \exp(i\varphi_n)$, with A_n and φ_n denote the amplitude and phase of each element, respectively, and t_{mn} is the elements of transmission matrix representing the propagation of light through the optical system. According to the feedback-based wavefront shaping, a desired output field is generated after imposing a proper phase map on the incident light. We define the desired focus pattern in the output field as the focus area. To modulate the random speckle into a uniform focal spot with designed pattern, we introduced two parameters, namely the intensity enhancement η describing the intensity magnitude of the focal spot, and the coefficient of variation (cv) characterizing the uniformity of the intensity distribution of the focal spot, which expresses the intensity fluctuation of the focus area. The

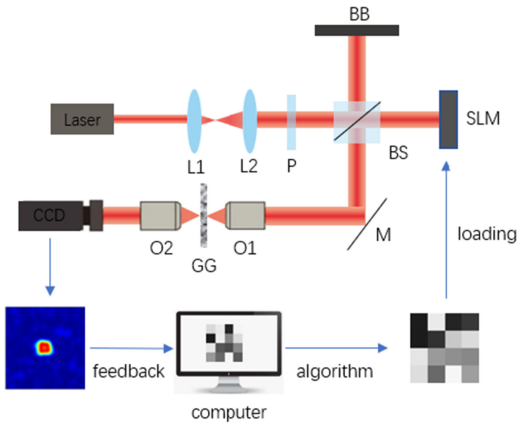

Fig. 1. Experimental setup of feedback-based wavefront shaping. L1, L2: lens. P: polarizer. BS: beam splitter. SLM: spatial light modulator. BB: beam block. M: mirror. O1, O2: objective lenses. GG: ground glass. CCD: charge coupled device.

definitions of these two parameters are as follows:

$$\eta = \frac{< I_{obj} >}{< I_{initial} >}, \tag{2}$$

$$cv = \frac{\sigma_{obj}}{< I_{obj} >}, \tag{3}$$

where $< I_{obj} >$ is the average light intensity at the focus area, $< I_{initial} >$ denotes the average light intensity of the output speckle field before wavefront modulation, and σ_{obj} represents the standard deviation of all points in the focus area. As η increases, the intensity enhancement of the focal area increases. cv reflects uniformity of the intensity distribution of the focus area. Small cv values mean the intensity fluctuation of the focus area is low, implying a high uniformity of the focus area.

Cost function is applied to balance the weight between the intensity enhancement and uniformity of the focal area and is defined as:

$$C = \sum_{i=1}^{m} I_i - mf(\sigma_{obj})^2 / \langle I_{initial} \rangle, \tag{4}$$

where m is the number of points in focal area, I_i is the intensity of each focal point, $(\sigma_{obj})^2$ is the variance of the intensity of all focal points, and f is the parameter balancing the weight between the intensity enhancement and uniformity. A large f corresponds to high uniformity but low intensity enhancement, whereas a small f corresponds to a high intensity enhancement but poor uniformity. Therefore, an appropriate f must be selected to simultaneously achieve focal patterns with a large intensity enhancement and a high uniformity.

3. Generation of Focal Patterns By GA and HEA

The experimental setup is shown in Fig. 1. A laser beam with wavelength of 632.8 nm is emitted by He-Ne laser (HRS015B, THORLABS) and expanded by a couple of lenses L1 and L2. Given that horizontal linearly polarized illumination is required to realize the phase modulation, a polarizer is placed in front of the spatial light modulator (SLM; PLUTO-VIS, HOLOEYE). The SLM is operated in zeroth order. The phase modulated light from the SLM is focused on the ground glass (220grit-THORLABS) by an objective lens (20×, NA = 0.4). The diffused light is then collected by another objective lens (20×, NA = 0.4), and captured by a CCD camera (PROSILICA GT1910, AVT). In the experiment, the light collected by the CCD camera is adopted as the feedback of the algorithms.

An optimized phase map is then calculated and imposed on the beam by the SLM to generate a desired focal pattern.

As a widely-used global optimization algorithm, GA behaves robustly against disturbances. In the wavefront shaping, it computes an optimized phase map to modulate the speckle into a desired focal pattern. The first step of the GA is generating a random original population as the original phase map for the light field modulation. In each round of iteration, two phase maps in the population are selected as parents. The cost value calculated by the cost function is chosen as the fitness value during the GA modulation. A high fitness value indicates a great probability of being selected. The parents generate the offspring phase map after crossing and mutating. This process continues for G times and produces G offspring in each iteration. The original population and the offspring are sorted by fitness value, and NP phase maps with high fitness are selected as the new population. During iteration, the feature of the population with high fitness is preserved, indicating that a fully optimized phase map can be acquired. In this experiment, the f of the cost function is set as $f = 0.16$, and other parameters are: The size of initial population NP $= 32$, the generation or the number of iterations NG $= 256$, segment $N = 1024$, and the mutation rate of the offspring can be expressed by this formula: $R = (R_0 - R_{end}) \cdot \exp(-\frac{d}{p}) + R_{end}$, where $R_0 = 0.01$ is the initial mutation factor, $R_{end} = 0.0025$ is the final mutation factor, $p = 200$ is the decay factor, and d is the number of iterations.

Among several optimization algorithms, HEA performs excellently in wavefront modulation. Compared with continuous sequential algorithm [3], HEA can modulate half of the elements of the phase map in each iteration, indicating its efficient phase modulation and robustness. Compared with that of partitioning algorithm (PA) [29], although PA can modulate half of the elements of the phase map in each iteration like HEA, the phase element of HEA in each iteration process is not randomly selected but determined by series of Hadamard basis vectors. Each column of the Hadamard matrix is a Hadamard basis vector represented by $H_n(k)(k = 1, \cdots n^2)$, with n the order of the Hadamard matrix, and k the sequence number of the column. Given that the Hadamard basis vector is orthogonal to each other, any two basis vectors are linearly independent. Compared with PA, HEA can obtain greater intensity enhancement in a few iterations by reducing the redundant information during modulation. In each iteration, the corresponding sequence 2D Hadamard basis vector is loaded in SLM to modulate the phase map. Except for the first column in the Hadamard matrix, the value of half elements of each Hadamard basis vector is "-1", and the value of remaining half elements is "+1". The value can be transformed to "0" and "+1"by adopting the operation $(H_n(k) + 1)/2$. Four-step phase shift is then applied to calculate the retardation angle of the "0" and "+1" part. In this process, the "0" part without phase modulation is set as reference light, and the additional phase modulation of 0, $\pi/2$, π and $3\pi/2$ is imposed on the "+1" part. The retardation angle φ between the reference part and modulation part can be calculated with phase-modulated intensities as:

$$\varphi = Arg[(I_1 - I_3) + i(I_2 - I_4)], \tag{5}$$

where I_i represents the intensity in i-th step phase shift and $Arg()$ calculates the phase angle. After φ is added to the "+1" part, the retardation angle between the phase-shifted light and the reference light is compensated. Hence, a coherent superposition is formed at the target focus point. Consequently, the best phase map in this iteration is obtained. This process is repeated until all the Hadamard basis vectors are loaded and the optimal modulation map is obtained. Fig. 2 utilizes a 4*4 Hadamard matrix as an example to illustrate principle of HEA. In this experiment, $f = 0.08$ is selected for HEA. The Hadamard basis is from 32*32 Hadamard matrix, which means the modulate segment of $N = 1024$.

Figs 3(a), (b), and (c) show the speckle field before modulation and the intensity distribution after modulation with GA and HEA. The designed focal pattern is a 11*11 square region. GA and HEA can modulate the speckle field into a specific focal pattern. The evolution of enhancement and coefficient of variation during the measurements indicate that HEA can generate a bright focal

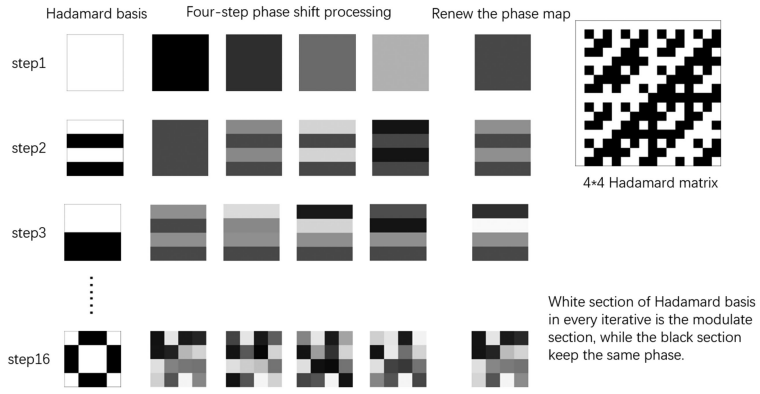

Fig. 2. The schematic diagram of HEA.

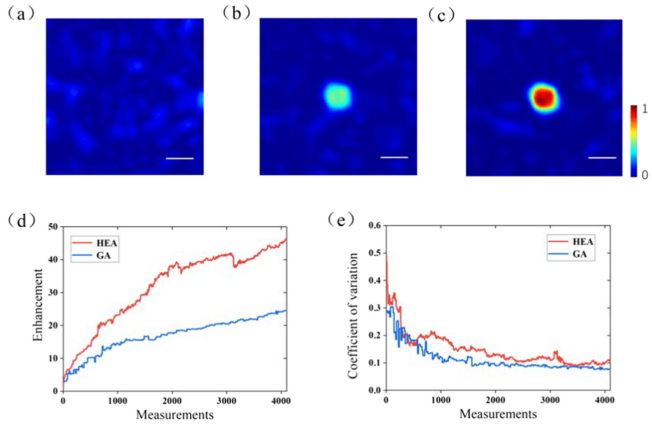

Fig. 3. The performance of the GA and HEA on speckle modulation. (a): the speckle field before modulation. (b): focal pattern after 1024 iterations of GA modulation. (c): focal patter after 1024 iterations of HEA modulation. (d): the evolution of intensity enhancement of GA (blue) and HEA (orange). (e): The evolution of coefficient of variation of intensity of GA (blue) and HEA (orange). The scale bar is 100 μm.

pattern, and GA can achieve high uniformity as shown in Figs. 3(e) and 3(f), respectively. Four-step phase shift is employed in HEA to achieve the constructive interference in the target region. Therefore, HEA can obtain a focal pattern with large intensity enhancement but weak uniformity. For GA, the cost function is the only discriminant for calculating the fitness value of each individual in the population. This function directly determines the selection of the optimal individual and new population in each iteration. Therefore, the magnitude and the uniformity of the intensity in the target area in each round are strictly limited by the cost function. Compared with HEA, GA has better uniformity during modulation.

4. Generation of Uniform Focal Patterns by HGA

In consideration of the superiority of GA and HEA on intensity uniformity and intensity enhancement, respectively, a hybrid algorithm combining the advantages of these two algorithms is proposed. The hybrid algorithm named HGA can be divided into two steps: (1) running HEA to generate a focal pattern with high enhancement and selecting the phase maps in the last 100 iterations that can generate a focal pattern with high enhancement; and (2) sorting the selected 100 phase maps according to the fitness value, choosing the 50 phase maps with large fitness value as the original population of GA, and running GA until the output condition is reached. Fig. 4 depicts the flow chart of HGA. The merit of HGA is adopting the optimized phase maps from HEA

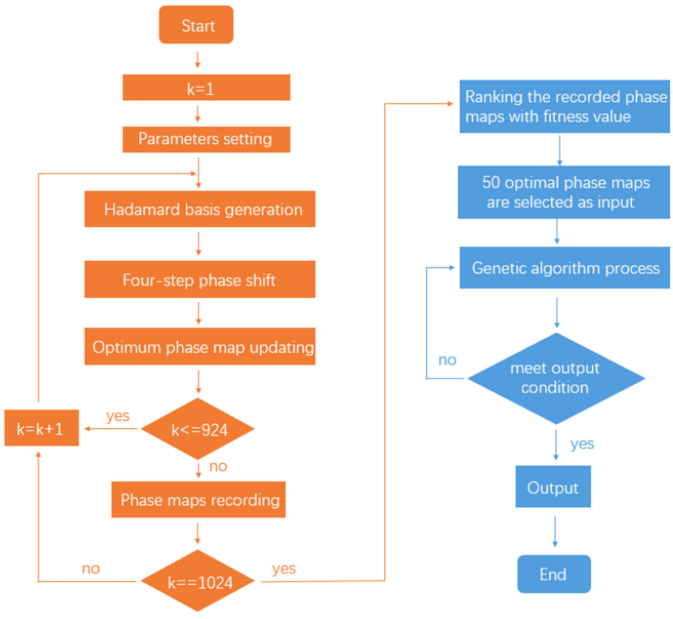

Fig. 4. The flow chart of HGA.

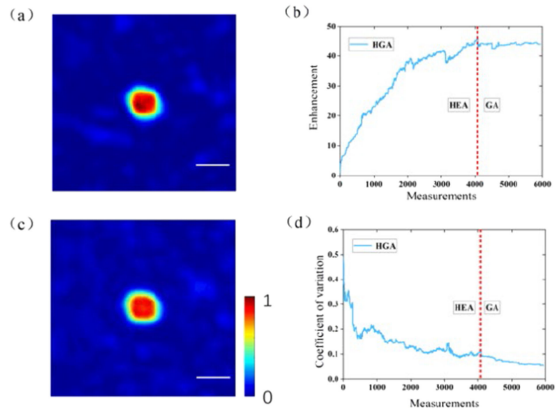

Fig. 5. Generation of uniform focal pattern by HEA and HGA modulation. (a): the intensity distribution after HEA modulation. (b): the evolution of intensity enhancement of HGA modulation. (c): the intensity distribution after HGA modulation. (d): the evolution of coefficient of variation of HGA modulation. The red dotted line is the junction of HEA and GA in HGA. The scale bar is 100 μm.

as the original population of GA. The optimized phase maps generated by HEA can generate a bright focal pattern. The uniformity of the focal pattern is improved by running the GA. Finally, a focal pattern with high intensity enhancement and perfect uniformity can be achieved.

Modulating the speckle into a square uniform focal pattern is taken as an example to illustrate the performance of the proposed HGA algorithm. The results are presented in Fig. 5. A preliminary focal pattern (Fig. 5(a)) is generated by running HEA. The fluctuation of intensity is suppressed (Fig. 5(b)) by further applying the GA. The evolution of the enhancement and the coefficient of variation are presented in Figs.5(b) and (d), respectively. With HEA running, the intensity enhancement increases gradually, and the coefficient of variation decreases and then reaches saturation point. After GA running, the intensity enhancement keeps nearly invariant, but the coefficient of variation drops gradually. These curves verify that, at the expense of negligible light intensity enhancement reduction, the uniformity can be improved significantly.

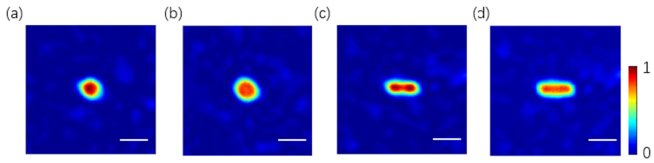

Fig. 6. Generation of different focal patterns with HGA. (a) and (b) the circular focal pattern by applying HEA and HGA modulation, respectively. (c) and (d) are the rectangular focal pattern by applying HEA and HGA modulation, respectively. The scale bar is 100 μm.

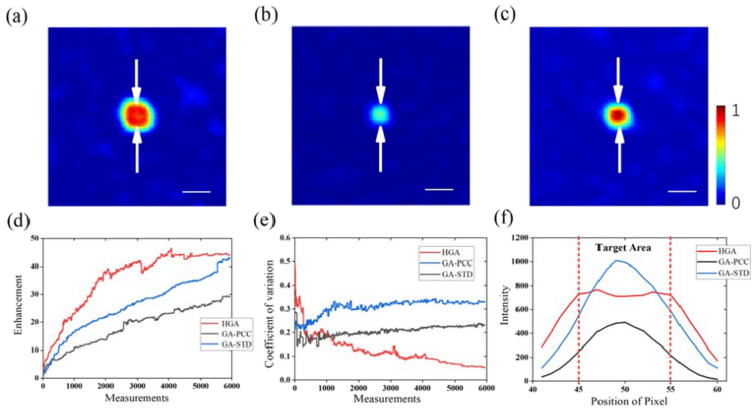

Fig. 7. The comparison between HGA modulation and GA-PCC and GA-STD. (a), (b) and (c): the intensity distribution of focal patterns generated by HGA, GA-PCC, and GA-STD after 5946 iterations; (d): the evolution of enhancement of three algorithms; (e): the evolution of coefficient of variation of three algorithms. (f): the intensity profiles between two arrows in Fig. 7. (a), (b), and (c). The scale bar is 100 μm.

Fig. 6 shows additional examples of the modulation by HGA. One is a circular focal pattern, and the other one is a rectangular focal pattern. Figs. 6(a) and 6(c) are the results after applying the HEA on the speckle modulation. The uniformity of these two focal spots is improved by further applying the GA as shown in Figs. 6(b) and 6(d). These experimental results also verify the superiority of HGA in the generation of a uniform focal pattern with high intensity enhancement.

GA has been utilized to modulate the speckle into a desired pattern. PCC and a standard-deviation-based expression have been introduced as the cost function of the iterative algorithm [20]–[21]. These two methods are referred to as GA-PCC and GA-STD, respectively. Their performance in the generation of uniform focal pattern were compared with that of the proposed HGA. Figs 7(a), (b), and (c) are the modulated intensity distribution of HGA, GA-PCC, and GA-STD, respectively, after 5946 measurements. The evolution of the intensity enhancement during the iteration (Fig. 7d) indicates that the enhancement of HGA is similar to that of GA-STD, whereas that of GA-PCC is lower than those of the other two algorithms. Although GA-STD and HGA exhibit strong ability for intensity enhancement, the uniformity of GA-STD is worse than that of HGA as presented in Fig. 7e. The intensity profiles shown in Fig. 7f reveal that the profiles of GA-STD and GA-PCC follow Gaussian distribution rather than a flattop distribution.

5. Conclusion

The HGA algorithm is proposed to generate the focal patterns with high intensity enhancement and excellent uniformity. On the basis of the performance of GA and HEA in the generation of uniform focal spots, HEA generates focal patterns with high intensity enhancement, and GA obtains uniform intensity. The proposed HGA combines the advantages of these two algorithms as well as inherits both high intensity enhancement of HEA and the high uniformity of GA. Compared with GA-STD and GA-PCC, HGA shows superiority in generating focal patterns with strong intensity and uniform

distribution. The superior performance of HEA in the generation of uniform focal patterns from speckle opens novel avenues for laser manufacturing and medical treatment.

Disclosures

The authors declare no conflicts of interest.

References

[1] D. B. Phillips *et al.*, "Shape-induced force fields in optical trapping," *Nature Photon.*, vol. 8, no. 5, pp. 400–405, 2014.
[2] Q. Zhan, "Cylindrical vector beams: From mathematical concepts to applications," *Adv. Opt. Photon.*, vol. 1, no. 1, pp. 1–57, 2009.
[3] M. Vellekoop and A. P. Mosk, "Focusing coherent light through opaque strongly scattering media," *Opt. Lett.*, vol. 32, no. 16, pp. 2309–2311, 2007.
[4] L. Chen, R. K. Singh, Z. Chen, and J. Pu, "Phase shifting digital holography with the Hanbury Brown-Twiss approach," *Opt. Lett.*, vol. 45, no. 1, pp. 212–215, 2020.
[5] L. Chen, Z. Chen, R. K. Singh, and J. Pu, "Imaging of polarimetric-phase object through scattering medium by phase," *Opt. Exp.*, vol. 28, no. 6, pp. 8145–8155, 2020.
[6] H. P. Paudel, C. Stockbridge, J. Mertz, and T. Bifano, "Focusing polychromatic light through strongly scattering media," *Opt. Exp.*, vol. 21, no. 14, pp. 17299–17308, 2013.
[7] Y. F. Guan, O. Katz, E. Small, J. Y. Zhou, and Y. Silberberg, "Polarization control of multiply scattered light through random media by wavefront shaping," *Opt. Lett.*, vol. 37, no. 22, pp. 4663–4665, 2012.
[8] W. Fan, Z. Chen, V. V. Yakovlev, and J. Pu, "High-fidelity image reconstruction through multimode fiber via polarization-enhanced parametric speckle imaging," *Laser Photon. Rev.*, vol. 15, 2021, Art. no. 2000376.
[9] E. Small, O. Katz, Y. F. Guan, and Y. Silberberg, "Spectral control of broadband light through random media by wavefront shaping," *Opt. Lett.*, vol. 37, no. 16, pp. 3429–3431, 2012.
[10] L. Wan, X. Ji, R. K. Singh, Z. Chen, and J. Pu, "Use of scattering layer as a programmable spectrum filter," *IEEE J. Quantum Electron.*, vol. 55, no. 5, 2019, Art. no. 6100306.
[11] E. S. Katz, Y. Bromberg, and Y. Silberberg, "Focusing and compression of ultrashort pulses through scattering media," *Nature Photon.*, vol. 5, no. 6, pp. 372–377, 2011.
[12] J. Aulbach, B. Gjonaj, P. M. Johnson, A. P. Mosk, and A. Lagendijk, "Control of light transmission through opaque scattering media in space and time," *Phys. Rev. Lett.*, vol. 106, no. 10, 2011, Art. no. 103901.
[13] M. Vellekoop and A. P. Mosk. "Universal optimal transmission of light through disordered materials," *Phys. Rev. Lett.*, vol. 101, no. 12, 2008, Art. no. 120601.
[14] I. Freund, "Looking through walls and around corners," *Physica A*, vol. 168, no. 1, pp. 49–65, 1990.
[15] M. V. van Rossum and T. M. Nieuwenhuizen, "Multiple scattering of classical waves: Microscopy, mesoscopy, and diffusion," *Rev. Mod. Phys.*, vol. 71, no. 1, pp. 313–371, 1999.
[16] M. W. Matthès, P. del Hougne, J. de Rosny, G. Lerosey, and S. M. Popoff, "Optical complex media as universal reconfigurable linear operators," *Optica*, vol. 6, no. 4, pp. 465–472, 2019.
[17] Y. Choi *et al.*, "Overcoming the diffraction limit using multiple light scattering in a highly disordered medium," *Phys. Rev. Lett.*, vol. 107, no. 2, 2011, Art. no. 023902.
[18] E. G. van Putten, D. Akbulut, J. Bertolotti, W. L. Vos, A. Lagendijk, and A. P. Mosk, "Scattering lens resolves sub-100nm structures with visible light," *Phys. Rev. Lett.*, vol. 106, no. 19, 2011, Art. no. 193905.
[19] D. B. Conkey, A. N. Brown, A. M. Caravaca-Aguirre, and R. Piestun, "Genetic algorithm optimization for focusing through turbid media in noisy environments," *Opt. Exp.*, vol. 20, no. 5, pp. 4840–4849, 2012.
[20] D. B. Conkey and R. Piestun, "Color image projection through a strongly scattering wall," *Opt. Exp.*, vol. 20, no. 25, pp. 27312–27318, 2012.
[21] L. Wan, Z. Chen, H. Huang, and J. Pu, "Focusing light into desired patterns through turbid media by feedback-based wavefront shaping," *Appl. Phys. B*, vol. 122, no. 7, pp. 204, 2016.
[22] Q. Feng, F. Yang, X. Xu, B. Zhang, Y. Ding, and Q. Liu, "Multi-objective optimization genetic algorithm for multi-point light focusing in wavefront shaping," *Opt. Exp.*, vol. 27, no. 25, pp. 36459–36473, 2019.
[23] T. Peng *et al.*, "Real-time optical manipulation of particles through turbid media," *Opt. Exp.*, vol. 27, no. 4, pp. 4858–4866, 2019.
[24] A. Hedayat and W. D. J. T. A. O. S. Wallis, "Hadamard matrices and their applications," *Ann. Statist.*, vol. 6, no. 6, pp. 1184–1238, 1978.
[25] J. Seberry, B. Jwysocki, and T. Awysocki, "On some applications of Hadamard matrices," *Metrika*, vol. 62, no. 2, pp. 221–239, 2005.
[26] Z. Wu, J. Luo, Y. Feng, X. Guo, Y. Shen, and Z. Li, "Controlling 1550-nm light through a multimode fiber using a hadamard encoding algorithm," *Opt. Exp.*, vol. 27, no. 4, pp. 5570–5580, 2019.
[27] J. Luo *et al.*, "Efficient glare suppression with Hadamard-encoding-algorithm-based wavefront shaping," *Opt. Lett.*, vol. 44, no. 16, pp. 4067–4070, 2019.
[28] B. Blochet, L. Bourdieu, and S. Gigan, "Focusing light through dynamical samples using fast continuous wavefront optimization," *Opt. Lett.*, vol. 42, no. 23, pp. 4994–4997, 2017.
[29] M. Vellekoop and A. P. Mosk, "Phase control algorithms for focusing light through turbid media," *Opt. Commun.*, vol. 281, no. 11, pp. 3071–3080, 2008.